Association Between Geographic Atrophy Progression and Reticular Pseudodrusen in Eyes With Dry Age-Related Macular Degeneration

Marcela Marsiglia,[1–4] Sucharita Boddu,[1] Srilaxmi Bearelly,[2] Luna Xu,[5] Barry E. Breaux Jr,[5] K. Bailey Freund,[1–4] Lawrence A. Yannuzzi,[1,3,4] and R. Theodore Smith[1]

[1]Department of Ophthalmology, New York University Langone Medical Center, New York, New York
[2]Department of Ophthalmology, Columbia University, New York, New York
[3]Vitreous Retina Macula Consultants of New York, New York, New York
[4]LuEsther T. Mertz Retinal Research Center, Manhattan Eye, Ear and Throat Hospital, New York, New York
[5]Columbia University College of Physicians and Surgeons, New York, New York

Correspondence: R. Theodore Smith, Department of Ophthalmology, New York University Langone Medical Center, 462 First Avenue - NBV 5N18, New York, NY 10016; roland.smith@nyumc.org.

Submitted: October 2, 2012
Accepted: October 2, 2013

Citation: Marsiglia M, Boddu S, Bearelly S, et al. Association between geographic atrophy progression and reticular pseudodrusenen eyes with dry age-related macular degeneration. *Invest Ophthalmol Vis Sci.* 2013;54:7362–7369. DOI:10.1167/iovs.12-11073

Purpose. To evaluate geographic atrophy (GA) progression in eyes with dry AMD and to determine factors related to GA expansion, notably reticular pseudodrusen (RPD), also known as subretinal drusenoid deposits (SDD) or reticular macular disease (RMD).

Methods. This was a retrospective cohort study of patients with dry AMD who were diagnosed with GA in at least one eye and were imaged with sequential fundus autofluorescence (FAF) and/or near infrared reflectance (NIR-R) imaging. Images were analyzed for the presence of GA within the macular region. Geographic atrophy progression was measured in the fields of a modified Wisconsin grid and spatially correlated with RPD. Factors also evaluated for association with GA progression included initial GA size and pattern.

Results. The study sample included 126 eyes of 92 patients, with an average follow up of 20.4 months (SD = 11.7). At baseline, 93.6% of eyes had RPD, and the average GA area was 2.8 mm^2 (SD = 2.9). The average GA progression rate was 0.8 mm^2/y (SD = 0.6), with a statistically significant difference between the unilobular and multilobular phenotype groups (0.3 mm^2/y vs. 0.9 mm^2/y, $P = 0.02$). Patients in the lower 50th percentile of initial GA area had a lower progression rate than patients in the upper 50th percentile (0.6 mm^2/y vs. 1.1 mm^2/y, $P < 0.001$). Geographic atrophy progression was more frequent in fields with RPD than in those without RPD (74.2% vs. 41.7%, $P < 0.001$).

Conclusions. The high correlation between the presence of RPD (also known as SDD or RMD) and the presence of GA, and the expansion of GA into areas with these lesions suggest that they are an early manifestation of the process leading to GA.

Keywords: geographic atrophy, age-related macular degeneration, reticular macular disease, reticular pseudodrusen, subretinal drusenoid deposits, autofluorescence, infrared

Age-related macular degeneration is the leading cause of central vision loss among adults in industrialized countries.[1,2] Age-related macular degeneration can be divided into early and late stages. The late stage of AMD can be further categorized as neovascular or dry (nonneovascular). While geographic atrophy (GA) may occur in both the neovascular and dry forms of AMD,[3] it is better characterized in the dry form. Proposed etiologic mechanisms for the development of GA include ischemia, senescence, oxidative and photo-oxidative damage, and inflammation, either directly or through apoptotic mechanisms.[4–6] Antioxidant vitamin therapy is the only treatment option currently available for early AMD, but, according to later analyses of the Age-Related Eye Disease Study, it shows no beneficial effect on GA progression rate.[7] There is still no proven effective treatment for atrophy. Thus, the investigation of clinical factors related to the development and growth of atrophic lesions in an effort to stop or retard this process is vital to expediting the search for treatment of AMD-related atrophy.

The most important histopathologic feature associated with atrophy is death of affected RPE cells.[8] When these cells die, all of their contents disappear, resulting in the characteristic GA pattern identifiable in various imaging modalities. In color fundus photography, GA is specifically attributed to the disappearance of melanin from RPE cells, resulting in a distinct area of decreased pigmentation and improved visualization of underlying choroidal vessels.[9] Visualization of underlying choroidal vessels is also possible when using near infrared reflectance (NIR-R) images, in which GA is characterized by areas of hyperreflectance that are observed as brighter areas. The presentation of GA in fundus autofluorescence (FAF) images is attributed to the disappearance of lipofuscin from RPE cells. The autofluorescence normally emitted by RPE lipofuscin upon stimulation is consequently absent, resulting in areas of hypoautofluorescence or absent autofluorescence,

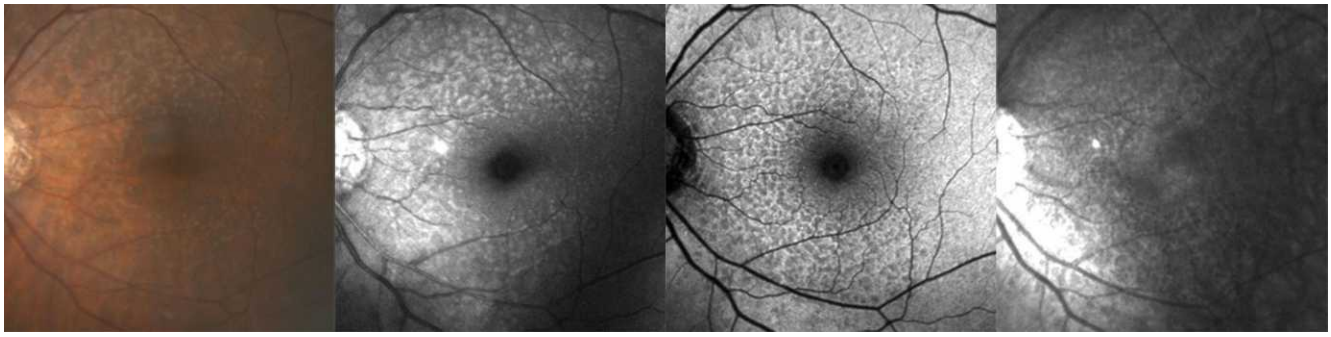

FIGURE 1. From *left* to *right*, the classical presentation of reticular pseudodrusen is shown in different imaging modalities: *yellow* or *light* interlacing networks ranging from 125 to 250 μm in width are seen in color fundus photography and red-free imaging, respectively. Hypoautofluorescent lesions against a background of elevated autofluorescence are observed in autofluorescence imaging. Hyporeflectant lesions against a background of hyperreflectance are seen in infrared imaging.

which are seen as darker areas.[10–15] Geographic atrophy also includes loss of the choriocapillaris, and the determination of its pathophysiology is very complex.

Reticular pseudodrusen (RPD) were first described in patients with AMD in 1990 as a peculiar yellowish pattern in the macular region (Fig. 1). They were also called "les pseudodrusen bleus" because of their enhanced visibility with the use of blue light.[16] Since then, numerous imaging modalities have been used to investigate this pattern. Using color fundus photographs, an ill-defined network of broad, interlacing yellowish lesions occurring mainly in the outer macula was identified. These lesions were considered a separate entity (a type of drusen referred to as "reticular drusen") in the Wisconsin Age-Related Maculopathy Grading System.[17] In 1995, a histopathologic analysis of RPD was published by Arnold et al.[15] This study demonstrated a significant loss of the middle choroidal layer of small vessels and increased spacing between the large choroidal veins and led to a new etiologic hypothesis for RPD: a fibrotic replacement of the choroidal stroma and loss of vascularity are responsible for the development of RPD, which may be a marker for choroidal ischemia.[15]

Improved imaging and visualization of RPD have been possible due to advances in imaging technology, particularly scanning laser ophthalmoscopy (SLO). Unlike soft drusen, these lesions have been observed to be hypofluorescent in the mid-to-late phases of indocyanine green angiography (ICGA)[18] and to correspond to a well-defined reticular pattern visualized with FAF imaging.[19] The term "reticular macular disease" (RMD) was introduced in 2009 and was defined to include RPD identified in color fundus photography, a reticular pattern seen in SLO imaging, or both.[20] The characteristic appearances of RPD in different imaging modalities are shown in Figure 1.[21]

In 2010, Zweifel et al.[22] proposed an anatomic theory to explain the appearance of RPD in advanced retinal imaging that was different than the vascular theories previously proposed. Using spectral domain optical coherence tomography (SD-OCT), they identified deposits of drusenoid material between the RPE and inner segment/outer segment junction, which they named "subretinal drusenoid deposits" (SDD). These SD-OCT findings were correlated with histopathology.[22] In 2012, Querques et al.[23] reported that, on ICGA, reticular patterns were hypofluorescent and not overlying the large choroidal vessels and that iso/hyperfluorescent areas adjacent to reticular patterns corresponded on SD-OCT to subretinal deposits. They also reported that the choroidal thickness in a group with RPD was reduced compared with that in a control group. As a conclusion of their study, they hypothesized that derangement of the RPE because of underlying atrophy and fibrosis of the choroid could lead to the accumulation of photoreceptor outer segments above the RPE, creating subretinal deposits.[23] Since 2010, results have been presented to support both suspected etiologies for RPD, the presence of subretinal deposits and choroidal changes, as well as a combination of both mechanisms occurring simultaneously.

RPD are a known risk factor in age-related maculopathy,[15,24] which is often seen in conjunction with GA. In FAF imaging, RPD appear as a pattern of hypoautofluorescent lesions against a background of elevated autofluorescence.[15,20,24–26] In NIR-R imaging, RPD appear as hyporeflectant lesions against a background of hyperreflectance.[24]

This study was performed to evaluate GA progression as evidenced by FAF and NIR-R images in eyes with dry AMD and to determine factors related to GA expansion, among which we highlighted RPD.

METHODS

This was a retrospective cohort study in which subjects were selected from the patient population of a private group retina practice and from Columbia University Medical Center, both located in New York, New York. The study was approved by the Western Institutional Review Board, Olympia, Washington, and by the Columbia University institutional review board. The study adhered to the Health Insurance Portability and Accountability Act of 1996 and followed the tenets of the Declaration of Helsinki. An informed consent waiver was granted to allow retrospective analysis from both practices.

Inclusion criteria were a diagnosis of GA in at least one eye and a minimum of two sessions of FAF and/or NIR-R imaging at least 6 months apart within the study interval (January 2005 to October 2010). Exclusion criteria were media opacity that resulted in poor image quality, photographic artifacts, or history of choroidal neovascularization, macular thermal laser photocoagulation, retinal vascular occlusion, retinal detachment, vitreoretinal or glaucoma surgery, RPE tear, macular hole, central serous chorioretinopathy, or high myopia (spherical equivalent greater than –6 diopters [D]). The baseline and final visit for each studied eye were respectively defined as the first and last visit with NIR-R and/or FAF images available within the study interval.

Each patient had undergone a minimum of two comprehensive ophthalmologic examinations by a retina specialist. As standard of care, the examination included evaluation of best-corrected visual acuity and acquisition of fundus (NIR-R and/or FAF) images using a confocal SLO (Heidelberg Retina Angiograph 2; Heidelberg Engineering, Heidelberg, Germany). Imaging in both modalities was performed using a 30° field

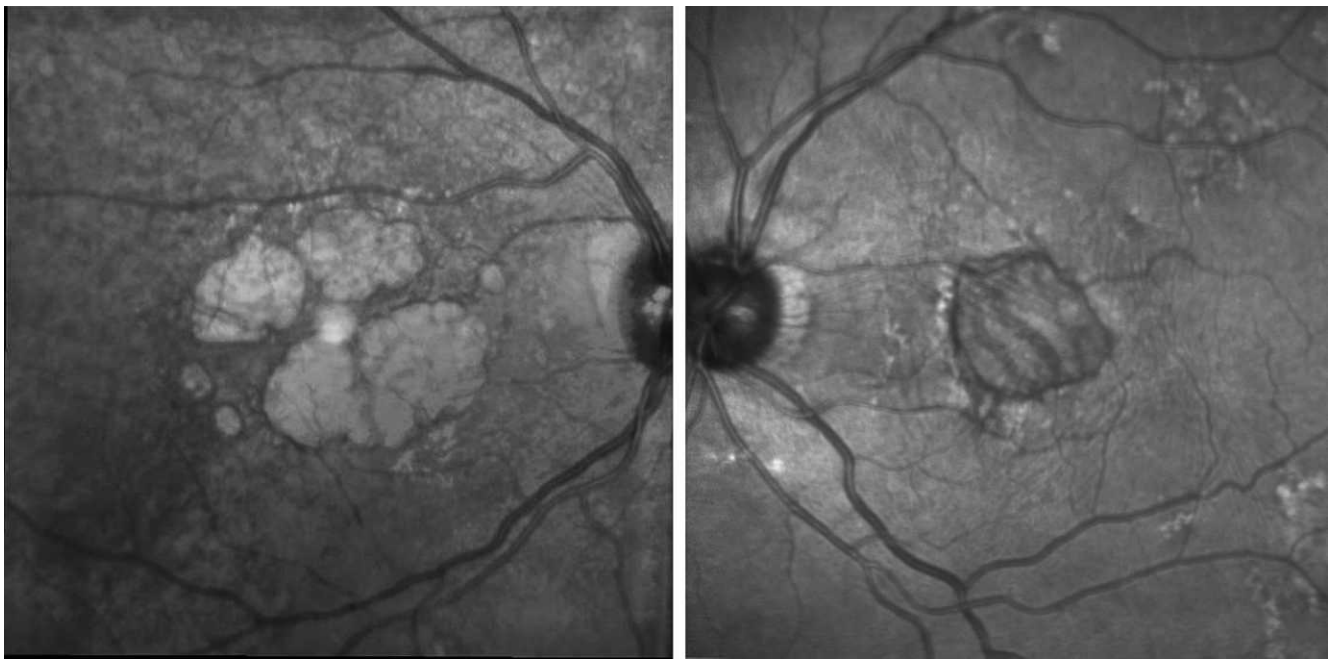

FIGURE 2. Typical NIR-R images of eyes with multilobular (*left*) and unilobular (*right*) GA. Images correspond to different patients.

of view at a resolution of 1536 pixels squared. Fundus autofluorescence images were obtained employing an optically pumped solid-state laser with an excitation wavelength of 488 nm and a barrier filter of 495 nm, and the standard acquisition protocol was followed. Fundus autofluorescence images encompassed the entire macular area (including at least a portion of the optic disc). Nine single images were averaged to produce a single frame with improved signal-to-noise ratio. Focus of the retinal image in the infrared reflection mode at an excitation wavelength of 820 nm was obtained for acquisition of at least nine single 30° NIR-R images. Demographic data (age and sex) and medical history, including hypertension, diabetes, and smoking (current smoker, past smoker, or never smoked), were collected for each patient. Each subject's visual acuity, refraction, and lens status (phakic, pseudophakic, or aphakic) were noted.

Geographic atrophy areas were identified on NIR-R as hyperreflective, well-delineated regions with increased visualization of choroidal vessels, and on FAF as regions with decreased or absent autofluorescence. Geographic atrophy was defined as a lesion measuring at least 300 μm in greatest linear diameter within the macula. Images acquired at baseline and final visit were selected for analysis. Serial images for each patient were registered,[27] and GA was measured in both NIR-R and FAF images using custom semiautomated software written in Matlab (Mathworks, Natick, MA).[28,29] Manual revision of the measured GA area was executed as needed. All measurements were performed independently by two graders (MM and SBo). In cases where there was a difference greater than 15% between measurements obtained by the two observers, arbitration through open adjudication was performed. In the few cases in which agreement was not achieved, a resolution was established by a third expert grader who evaluated the images (SBe). An average of the measurements of the two observers was used for statistical analysis. Areas of peripapillary atrophy were not classified as GA and accordingly were not included in GA measurements. In images that showed two or more distinct GA areas each measuring 300 μm or greater, each distinct area was measured and summed to generate the total GA area.

The calculated total area of GA was divided by the total image area (in mm^2) to give the percentage of GA in each image. The progression of GA from baseline to final visit was evaluated by calculating the GA growth rate per year, using the following formula:

$$\text{GA growth rate}\,(\text{mm}^2/\text{y}) = 12\times\frac{\text{GA size at final visit} - \text{GA size at baseline}}{\text{months of follow up}} \quad (1)$$

Each baseline image was also assessed for the presence or absence of RPD, which was identified as a pattern measuring at least 2-disc diameters of hypoautofluorescent lesions against a background of elevated autofluorescence in FAF images or hyporeflectant lesions against a background of hyperreflectance in NIR-R images. A modified Wisconsin grid was superimposed upon each baseline image, and the presence or absence of RPD was determined in five macular fields (superior, inferior, temporal, nasal, and central). The same modified Wisconsin grid was also superimposed upon each baseline and final visit image to determine the presence or absence of GA in all five macular fields. The images were then analyzed for GA growth; if there was an increase in GA area in a given field between baseline and final visit images, that field was categorized as a field of GA growth. In seven eyes, RPD status and GA growth were indeterminable in the central field because GA occupied that entire field at baseline; thus, central fields from these seven eyes were excluded from analysis. A correlation between fields of GA growth and the initial presence or absence of RPD in those fields was established.

Two GA phenotypic patterns, unilobular and multilobular, were defined as follows: unilobular GA was defined as a single (generally near-circular) area of atrophy, and multilobular GA was defined as two or more lobules of atrophy (Fig. 2). The FAF gray levels seen in lobules of multilobular cases were not required to be identical. These phenotypic patterns and initial

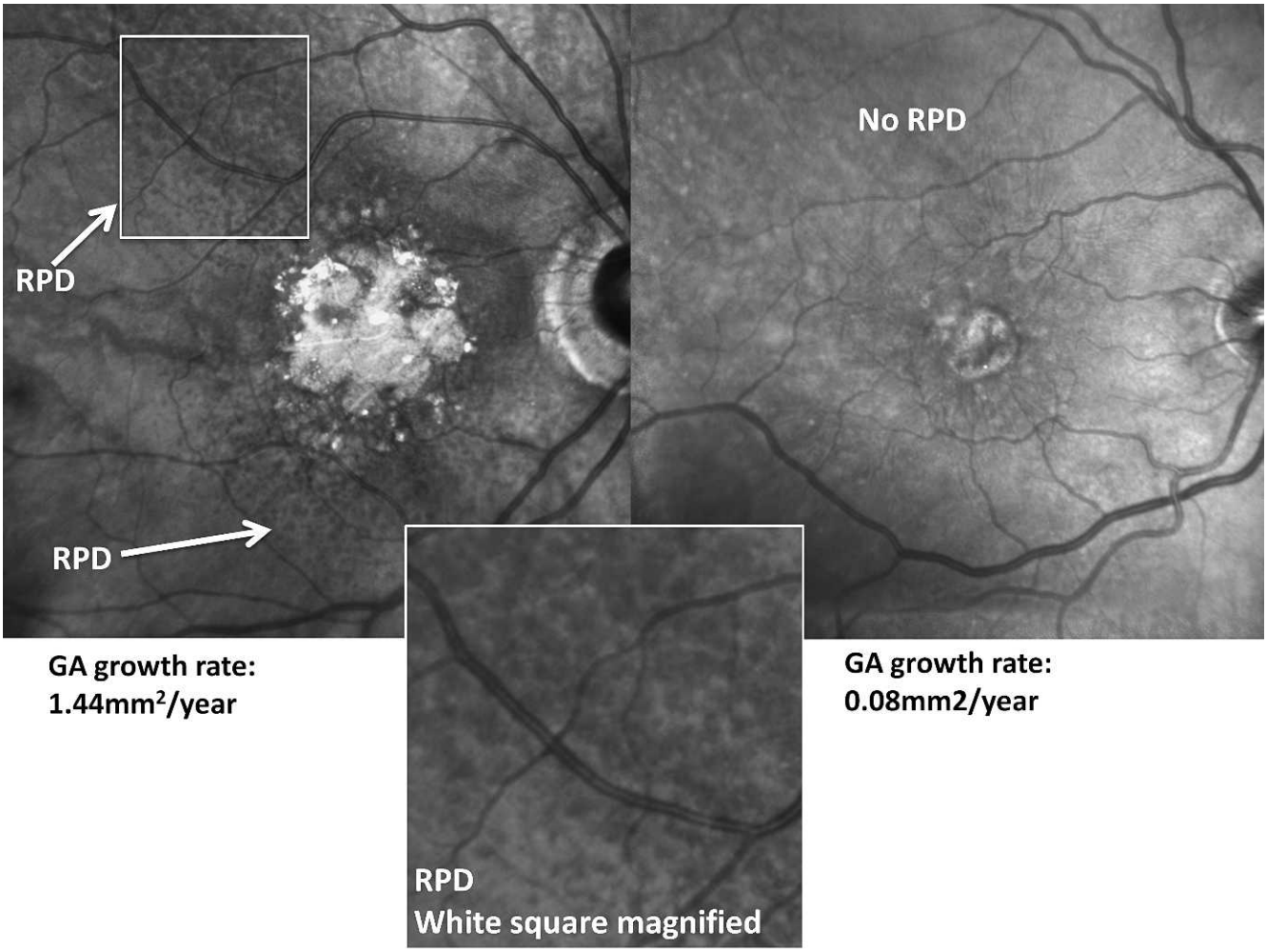

FIGURE 3. Baseline NIR-R images. An eye with RPD is shown on the *left*. *White arrows* point to RPD areas. A *white square box* is magnified *below*, showing the RPD pattern. An eye without RPD is shown on the *right*. The GA growth rate is shown at the *bottom* of each case.

GA lesion size were also analyzed for association with GA progression.

Statistical Analysis

Data was analyzed with descriptive statistics and inferential statistics. The χ^2 test was used to compare categorical outcomes, and the Student *t*-test was used to contrast quantitative variables. Statistical analysis was performed using Microsoft Excel 2011, version 14.0.0 (Microsoft, Redmond, WA). A *P* value less than 0.05 was considered statistically significant.

RESULTS

A total of 126 eyes of 92 patients were studied, of whom 69 (75.0%) were female. At baseline, subjects' ages ranged from 59 to 96 years, with a mean age of 81.9 years (SD = 6.7). The mean duration of follow up was 20.4 months (SD = 11.7). Among the 126 eyes, 118 eyes (93.6%) presented with RPD at baseline. At baseline, the average measured area of GA was 2.8 mm^2 (SD = 2.9). 97.5% of the eyes with RPD showed GA progression, which ranged from 0 to 2.9 mm^2/y. Eighty-seven and half percent of the eyes without RPD had GA progression, which ranged from 0 to 2.6 mm^2/y. The mean measured GA progression rate for all the eyes included in this study was 0.8 mm^2/y (SD = 0.6), with a statistically significant difference between the unilobular and multilobular groups (0.3 mm^2/y vs. 0.9 mm^2/y, $P = 0.02$). Most eyes with unilobular GA did not have RPD, while most eyes with multilobular GA did have RPD (28.6% with RPD vs. 97.5% with RPD, respectively). Figure 3 shows progression rates in an eye with RPD and an eye without RPD. Figure 4 exemplifies an eye with unilobular GA without RPD, as well as an eye with multilobular GA with concomitant RPD. Patients in the lower 50th percentile of initial measured GA area had a lower GA progression rate than patients in the upper 50th percentile (0.6 mm^2/y vs. 1.1 mm^2/y, $P < 0.001$). The studied eyes had a mean initial lesion size of 4.4 and 4.0 mm^2 in the multilobular and unilobular GA groups, respectively ($P = 0.14$). Sex did not prove to be a significant factor in GA progression rate (0.9 mm^2/y for females and 0.7 mm^2/y for males, $P = 0.28$). Likewise, age did not prove to be a significant factor in GA progression, as patients in the lower 50th percentile of age had a progression rate similar to that of patients in the upper 50th percentile (0.9 mm^2/y and 0.8 mm^2/y, respectively, $P = 0.13$). As illustrated in Figure 5, superimposition of a modified Wisconsin grid on baseline NIR-R and/or FAF images and determination of the presence or absence of RPD in each of the five macular fields showed RPD in the central field in 106 eyes (84.1%), in the superior field in 103 eyes (81.7%), in the temporal field in 83 eyes (65.9%), in the inferior field in 84 eyes (66.7%), and in the nasal field in 83

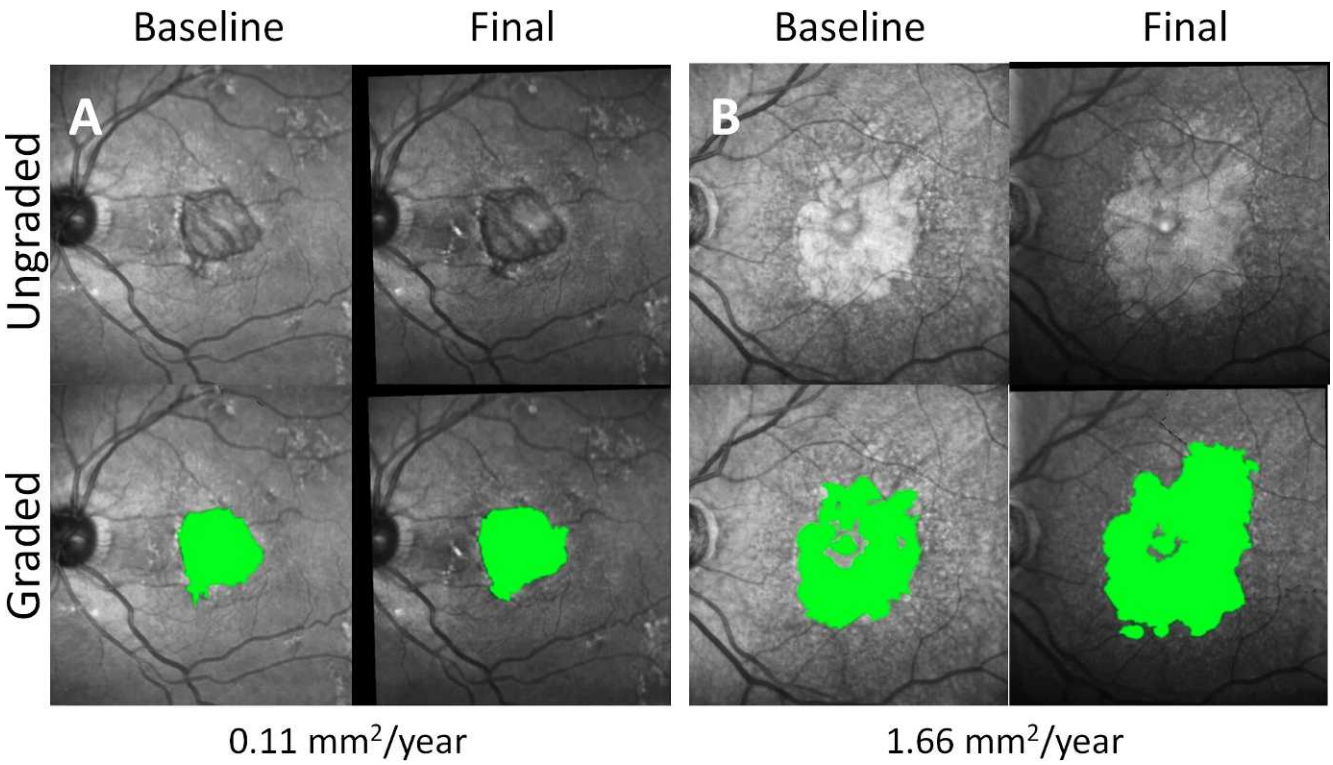

FIGURE 4. (**A**) Near infrared reflectance images of an eye with unilobular GA without RPD. (**B**) Near infrared reflectance images of an eye with multilobular GA, with lobules merging and RPD surrounding the atrophic area. *Top row*, ungraded images. *Bottom row*, graded images with areas of GA highlighted in *green*. The GA progression rate is shown at the *bottom* of each case.

eyes (65.9%). The Table summarizes the extent of RPD in the study sample, showing the total number of eyes without RPD (8, or 6.3%) and with RPD in one macular field (7, or 5.6%), two macular fields (14, or 11.1%), three macular fields (21, or 16.7%), four macular fields (26, or 20.6%), and five macular fields (50, or 39.7%).

For the quantitative correlation between RPD and GA growth, the five macular fields in each of the 126 included eyes contributed a total of 630 fields. A total of seven fields were deemed ungradable for RPD status and GA growth because GA occupied that entire field at baseline. Of the 623 gradable fields at baseline, 345 showed RPD, and 278 did not show RPD. Among those with RPD, 256 (74.2%) showed subsequent GA progression (i.e., increase in GA area between baseline and final images), and among those without RPD, 116 (41.7%) showed GA progression, corresponding to a statistically significant difference ($P < 0.001$).

DISCUSSION

The results of this study support a previously undescribed strong spatiotemporal association between RPD and GA progression in eyes with dry AMD. A previous detailed analysis of RPD, also known as subretinal drusenoid deposits or reticular macular disease, by Schmitz-Valckenberg et al.[30] has demonstrated that the presence of SDD on SD-OCT and the reticular pattern on NIR-R SLO are essentially equivalent. Thus, the main conclusions of the present study suggest a strong spatiotemporal association between SDD as seen with SD-OCT and GA progression, which should be kept in mind throughout the discussion.

The role of RPD in the progression of AMD generally is an important scientific question in the ophthalmic literature.[20,24,25,31] In this study, GA progressed significantly more often in areas previously manifesting these lesions than in areas that did not. One reason for this strong correlation could be a common underlying pathophysiology that initially causes the reticular pattern and subsequently drives the development of atrophy. Arnold et al.[15] related the presence of reticular drusen to abnormalities in the inner choroid. A relationship between AMD in general and concomitant degenerative changes in the choriocapillaris has also been demonstrated by Hayreh.[32,33] Blood flow studies in vivo performed by different scientists have shown impairment of choroidal circulation in AMD.[32–36] However, an association is still not proof of cause and effect. Indeed, GA can be a cause of choroidal atrophy (rather than a result). On the other hand, an elegant and recent 2-lesion 2-compartment model suggests that SDD lesions are a sign of RPE lipid recycling pathways resulting in a lipid and protein spill into the subretinal space, with ensuing photoreceptor damage and ultimately GA.[37] Hence, there is highly suggestive evidence for both anatomic theories. Recently, Querques et al.[23] have suggested that these may be complementary theories, hypothesizing that derangement of the RPE because of underlying atrophy and fibrosis of the choroid could lead to the accumulation of photoreceptor outer segments above the RPE, creating subretinal deposits.

Potential Relevance of GA Progression in Eyes With RPD

Both forms of late-stage AMD, neovascular and atrophic, have been associated with RPD.[24,38,39] The neovascular form has several treatment options currently available. Unfortunately, no efficacious treatment is available for the dry form, which means that it is important to study its possible causes and find future therapeutic targets. The strong relationship between GA and RPD shown herein suggests a similar etiology; therefore,

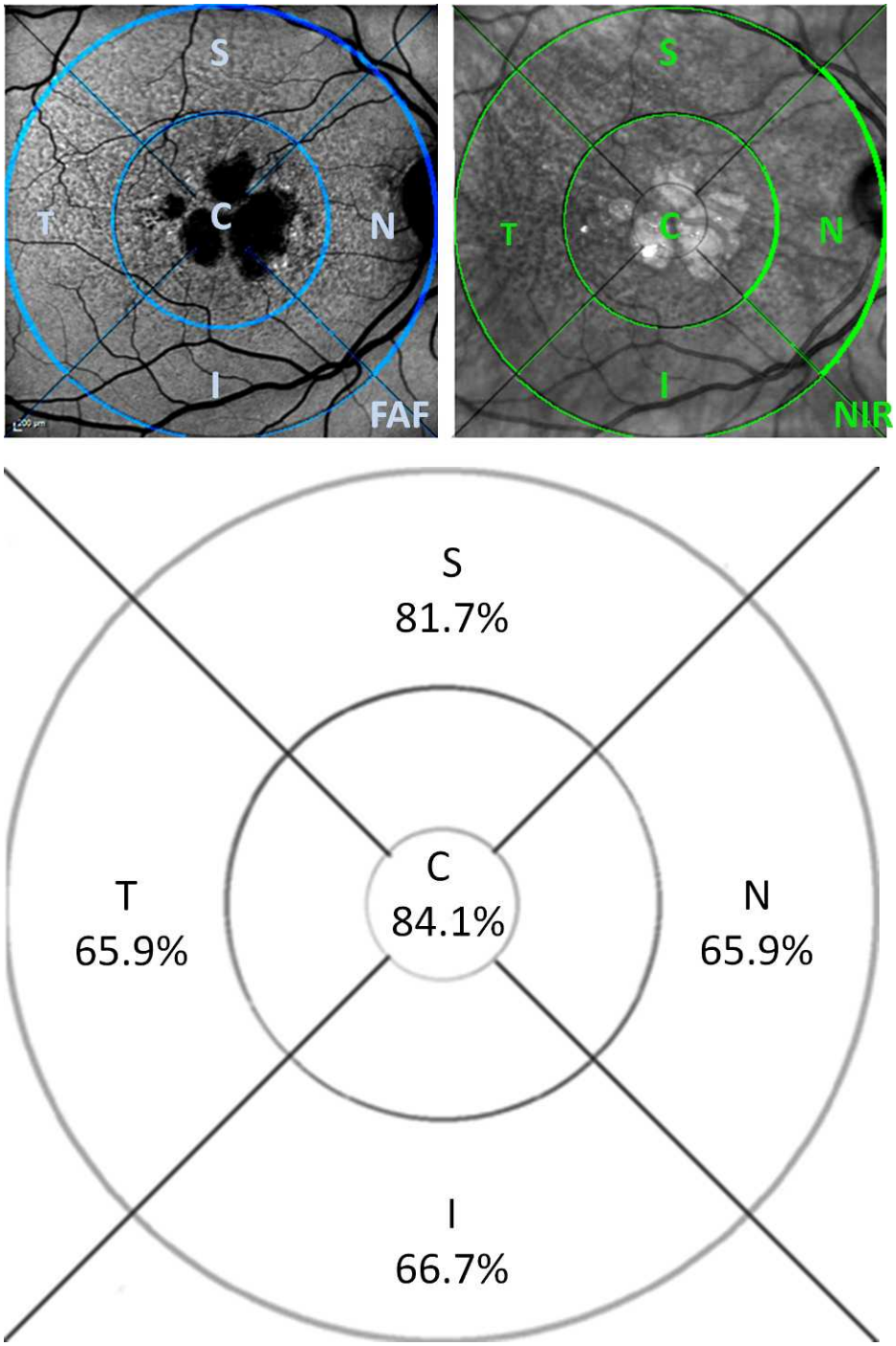

Figure 5. The *top row* shows examples of the modified Wisconsin grid superimposed on an autofluorescence image (*left*) and an (NIR-R) image (*right*) of an eye with multilobular GA and evident RPD. The considered fields of the grid are represented as C (central), N (nasal), S (superior), T (temporal), and I (inferior). The grid at the *bottom* shows the percentage of studied eyes that showed RPD in each field.

understanding the pathophysiology of RPD could be crucial to understanding and treating GA. An understanding of RPD could be within reach, despite the current controversy about the anatomy of the lesions themselves.[22,23,37,38,40]

GA Progression Rates

GA progression rates were found to be higher in eyes with a multilobular atrophic pattern (versus a unilobular pattern) or with larger initial lesion size. The multilobular atrophic pattern may reflect more widespread disease that leads in turn to a higher GA growth rate.[31–33,41] The faster progression rate in eyes with larger initial lesion size is consistent with other studies. However, the overall average GA progression rate of 0.8 mm^2/y found in this study was lower than in other reports, with rates ranging from 1.22 to 1.78 mm^2/y.[30,42–45] This may be due to the smaller initial average GA size of 2.8 mm^2 in our study.[42,43,45]

Table. Quantification of Eyes With Reticular Pseudodrusen in 0 to 5 Macular Fields of a Modified Wisconsin Grid

Number of Fields With RPD	Number of Eyes	Percentage of the Study Sample
RPD extent		
0	8	6.3
1	7	5.6
2	14	11.1
3	21	16.7
4	26	20.6
5	50	39.7
Total	126	100

Technological Advances in Identifying RPD and GA

Technological advances, particularly SLO imaging, may explain the much stronger association between RPD and GA found in this study than in past studies, which relied mainly on color fundus photographs for detection of RPD.[18] Previous studies, such as the report by Klein et al.,[24] have noted the same reason for improved detection of RPD. In addition, improved SLO image quality over time may have further improved recognition of RPD.[30]

Limitations and Strengths of the Study

The limitations of this study include its retrospective design. Prospective studies are indicated. Also, the study was not designed to analyze a possible correlation between GA and soft drusen. The eyes studied herein already had established GA and were not evaluated for the presence of pre-existing soft drusen. A longer natural history study, beginning with early AMD and including both soft drusen and RPD, would be of interest to compare and contrast these two paths to geographic atrophy. Another limitation was that image analysis was restricted to FAF and NIR-R modalities. However, as noted before, SDD on SD-OCT and the reticular pattern on NIR-R SLO are essentially equivalent.[30]

The strengths of this study include the large number of eyes, each having had a minimum of 6 months of follow up; the sensitivity of SLO imaging for RPD detection; and the semi-automated software used for GA quantification.

To the best of the authors' knowledge, this is the first study to report a strong spatiotemporal association between RPD and GA progression in the setting of dry AMD. Future prospective studies of RPD could help validate this observation. The correlation between these lesions and GA progression in dry AMD suggests that they are an early manifestation of the process leading to atrophy.

Acknowledgments

The authors thank Nicole M. Pumariega, MS, as a consultant on this project.

Supported by grants from the Robert Burch III Scholars Fund, Columbia University, New York, New York (SBe), National Institutes of Health/National Eye Institutes Grant R01 EY015520 (RTS), unrestricted funds from Research to Prevent Blindness (RTS), an individual investigator research award from the Foundation Fighting Blindness (RTS), and The Macula Foundation, Inc. (LAY and KBF).

Disclosure: **M. Marsiglia**, None; **S. Boddu**, None; **S. Bearelly**, None; **L. Xu**, None; **B.E. Breaux Jr**, None; **K.B. Freund**, Genentech, Inc. (F, C), Regeneron Pharmaceuticals, Inc. (C); **L.A. Yannuzzi**, None; **R.T. Smith**, None

References

1. Hyman L. Epidemiology of eye disease in the elderly. *Eye (Lond)*. 1987;1:330–341.
2. Friedman DS, O'Colmain BJ, Munoz, B, et al. Prevalence of age-related macular degeneration in the United States. *Arch Ophthalmol*. 2004;122:564–572.
3. Kumar N, Mrejen S, Fung AT, Marsiglia M, Loh BK, Spaide RF. Retinal pigment epithelial cell loss assessed by fundus autofluorescence imaging in neovascular age-related macular degeneration. *Ophthalmology*. 2013;120;334–341.
4. Zarbin MA. Current concepts in the pathogenesis of age-related macular degeneration. *Arch Ophthalmol*. 2004;122: 598–614.
5. Scholl HP, Fleckenstein M, Charbel Issa P, Keilhauer C, Holz FG, Weber BH. An update on the genetics of age-related macular degeneration. *Mol Vis*. 2007;13:196–205.
6. Kaneko H, Dridi S, Tarallo V, et al. DICER1 deficit induces Alu RNA toxicity in age-related macular degeneration. *Nature*. 2011;471:325–330.
7. Chew EY, Clemons TE, Agrón E, et al. Long-term effects of vitamins C and E, β-carotene, and zinc on age-related macular degeneration: AREDS report No. 35. *Ophthalmology*. 2013; 120:1604–1611.
8. Sarks JP, Sarks SH, Killingworth MC. Evolution of geographic atrophy of the retinal pigment epithelium. *Eye (Lond)*. 1988;2: 552–577.
9. Sunness JS, Bressler NM, Tian Y, Alexander J, Applegate CA. Measuring geographic atrophy in advanced age-related macular degeneration. *Invest Ophthalmol Vis Sci*. 1999;40:1761–1769.
10. Göbel AP, Fleckenstein M, Schmitz-Valckenberg S, Brinkmann CK, Holz FG. Imaging geographic atrophy in age-related macular degeneration. *Ophthalmologica*. 2011;226:182–190.
11. Spaide RF. Fundus autofluorescence and age-related macular degeneration. *Ophthalmology*. 2003;110:392–399.
12. Sunness JS, Ziegler MD, Applegate CA. Issues in quantifying atrophic macular disease using retinal autofluorescence. *Retina*. 2006;26:666–672.
13. Schmitz-Valckenberg S, Holz FG, Bird AC, Spaide RF. Fundus autofluorescence imaging: review and perspectives. *Retina*. 2008;28:385–409.
14. Khanifar AA, Lederer DE, Ghodasra JH, et al. Comparison of color fundus photographs and fundus autofluorescence images in measuring geographic atrophy area. *Retina*. 2012; 32:1884–1891.
15. Arnold JJ, Sarks SH, Killingsworth MC, Sarks JP. Reticular pseudodrusen: a risk factor in age-related maculopathy. *Retina*. 1995;15:183–191.
16. Mimoun G, Soubrane G, Coscas G. Macular drusen [in French]. *J Fr Ophtalmol*. 1990;13:511–530.
17. Klein R, Davis MD, Magli YL, Segal P, Klein BE, Hubbard L. The Wisconsin age-related maculopathy grading system. *Ophthalmology*. 1991;98:1128–1134.
18. Arnold JJ, Quaranta M, Soubrane G, Sarks SH, Coscas G. Indocyanine green angiography of drusen. *Am J Ophthalmol*. 1997;124:344–356.
19. Lois N, Owens SL, Coco R, Hopkins J, Fitzke FW, Bird AC. Fundus autofluorescence in patients with age-related macular degeneration and high risk of visual loss. *Am J Ophthalmol*. 2002;133:341–349.
20. Smith RT, Sohrab MA, Busuioc M, Barile G. Reticular macular disease. *Am J Ophthalmol*. 2009;148:733–743.
21. Martillo MA, Marsiglia M, Lee MD, Pumariega N, Bearelly S, Smith T. Is reticular macular disease a choriocapillaris perfusion problem? *Med Hypothesis Discov Innovation Ophthalmol J*. 2012;1:37–41.

22. Zweifel SA, Spaide RF, Curcio CA, Malek G, Imamura Y. Reticular pseudodrusen are subretinal drusenoid deposits. *Ophthalmology*. 2010;117:303–312, e1.
23. Querques G, Querques L, Forte R, Massamba N, Coscas F, Soured EH. Choroidal changes associated with reticular pseudodrusen. *Invest Ophthalmol Vis Sci*. 2012;53:1258–1263.
24. Klein R, Meuer SM, Knudtson MD, Iyengar SK, Klein BE. The epidemiology of retinal reticular drusen. *Am J Ophthalmol*. 2008;145:317–326.
25. Schmitz-Valckenberg S, Alten F, Steinberg JS, et al. Reticular drusen associated with geographic atrophy in age-related macular degeneration. *Invest Ophthalmol Vis Sci*. 2011;52:5009–5015.
26. Smith RT, Chan JK, Busuoic M, Sivagnanavel V, Bird AC, Chong NV. Autofluorescence characteristics of early, atrophic, and high-risk fellow eyes in age-related macular degeneration. *Invest Ophthalmol Vis Sci*. 2006;47:5495–5504.
27. Chen J, Smith R, Tian J, Laine AF. A novel registration method for retinal images based on local features. *Conf Proc IEEE Eng Med Biol Soc*. 2008;2008:2242–2245.
28. Lee N, Laine AF, Smith RT. Bayesian transductive Markov random fields for interactive segmentation in retinal disorders. *IFMBE Proc*. 2009;25:227–230.
29. Lee N, Smith RT, Laine AF. Interactive segmentation for geographic atrophy in retinal fundus images. *Conf Rec Asilomar Conf Signals Syst Comput*. 2008;2008:655–658.
30. Schmitz-Valckenberg S, Steinberg JS, Fleckenstein M, Visvalingam S, Brinkmann CK, Holz FG. Combined confocal scanning laser ophthalmoscopy and spectral-domain optical coherence tomography imaging of reticular drusen associated with age-related macular degeneration. *Ophthalmology*. 2010;117:1169–1176.
31. Klein R, Meuer SM, Knudtson MD, Klein BE. The epidemiology of progression of pure geographic atrophy: the Beaver Dam Eye Study. *Am J Ophthalmol*. 2008;146:692–699.
32. Hayreh SS. Posterior ciliary artery circulation in health and disease: the Weisenfeld lecture. *Invest Ophthalmol Vis Sci*. 2004;45:749–757; 748.
33. Hayreh SS. Macular lesions secondary to choroidal vascular disorders. *Int Ophthalmol*. 1983;6:161–170.
34. Hayreh SS. Controversies on submacular choroidal circulation. *Ophthalmologica*. 1981;183:11–19.
35. Foos RY, Trese MT. Chorioretinal juncture. Vascularization of Bruch's membrane in peripheral fundus. *Arch Ophthalmol*. 1982;100:1492–1503.
36. Anderson DH, Radeke MJ, Gallo NB, et al. The pivotal role of the complement system in aging and age-related macular degeneration: hypothesis re-visited. *Prog Retin Eye Res*. 2010;29:95–112.
37. Curcio CA, Messinger JD, Sloan KR, McGwin G, Medeiros NE, Spaide RF. Subretinal drusenoid deposits in non-neovascular age-related macular degeneration: morphology, prevalence, topography, and biogenesis model. *Retina*. 2013;33:265–276.
38. Pumariega NM, Smith RT, Sohrab MA, LeTien V, Souied EH. A prospective study of reticular macular disease. *Ophthalmology*. 2011;118:1619–1625.
39. Spaide RF, Armstrong D, Browne R. Continuing medical education review: choroidal neovascularization in age-related macular degeneration–what is the cause? *Retina*. 2003;23:595–614.
40. Sohrab MA, Smith RT, Salehi-Had H, Sadda SR, Fawzi AA. Image registration and multimodal imaging of reticular pseudodrusen. *Invest Ophthalmol Vis Sci*. 2011;52:5743–5748.
41. Hayreh SS. Segmental nature of the choroidal vasculature. *Br J Ophthalmol*. 1975;59:631–648.
42. Yehoshua Z, Rosenfeld PJ, Gregori G, et al. Progression of geographic atrophy in age-related macular degeneration imaged with spectral domain optical coherence tomography. *Ophthalmology*. 2011;118:679–686.
43. Holz FG, Bindewald-Wittich A, Fleckenstein M, et al. Progression of geographic atrophy and impact of fundus autofluorescence patterns in age-related macular degeneration. *Am J Ophthalmol*. 2007;143:463–472.
44. Bearelly S, Khanifar AA, Lederer DE, et al. Use of fundus autofluorescence images to predict geographic atrophy progression. *Retina*. 2011;31:81–86.
45. Lindblad AS, Lloyd PC, Clemons TE, et al. Change in area of geographic atrophy in the Age-Related Eye Disease Study: AREDS report number 26. *Arch Ophthalmol*. 2009;127:1168–1174.

Investigative Ophthalmology & Visual Science